Desalination and Water Treatment
www.deswater.com

doi: 10.1080/19443994.2015.1051129

57 (2016) 11255–11265
May

Taylor & Francis
Taylor & Francis Group

Kinetics and thermodynamic studies of phenol adsorption on nanocomposite

Meraj Alam Khan, Anees Ahmad*

Department of Chemistry, Aligarh Muslim University, Aligarh 202002, India, Tel. +9359754113; email: meraj.khan11@gmail.com (M. Alam Khan), Tel. +9536322688; email: ahmadanees17@yahoo.com (A. Ahmad)

Received 20 January 2015; Accepted 8 April 2015

ABSTRACT

An inorganic–organic hybrid nanocomposite materials has been used as a stable extractor for the removal of phenol and characterized using Fourier transform infrared (FTIR), and scanning electron microscopy (SEM) analyses. Batch adsorption experiments were employed to study the main parameters of kinetic study under various conditions (e.g. contact time, solution pH, initial metal ion concentration, temperature etc.). The most favourable pH for the optimum sorption of phenol was found to be 3–5. Langmuir and Freundlich isotherms were tested to describe the adsorption mechanism. The monolayer adsorption capacity of polyaniline Sn(IV) silicophosphate (PTSP) for phenol was found to be 3.76, 5.58 and 2.82 μg g^{-1} at 30, 40 and 50°C, respectively. Thermodynamic parameters were also computed and their results exposed the spontaneous and endothermic nature of sorption. FTIR confirmed that the interactions between phenol and PTSP were responsible for adsorption. SEM image showed the amorphous morphology of untreated PTSP. It was also found that after adsorption, the morphology of phenol-treated PTSP had been completely changed, which proved the phenomenon of adsorption. PTSP adsorbent has been successfully used for the removal of phenol from aqueous solutions.

Keywords: Inorganic–organic hybrid nanocomposite; Kinetic; Adsorption; Isotherm; Thermodynamic

1. Introduction

Phenols and phenolic compounds in wastewaters are hazardous organic pollutants which are of great environmental interest. Their determination has been increasing in recent years because of their toxicity, even at low concentrations. Phenolic compounds are often derived from various manufacturing processes such as pharmaceutical, oil refineries, coke plants and phenolic resin plants [1–5]. Discharge of phenolic waste may cause an unpleasant odour and flavour in concentration as low as 5 μg L^{-1} and are poisonous to aquatic life, plants and humans [6]. It has been reported that ingestion of phenols in concentrations from 10 to 240 mg L^{-1} for long periods causes mouth irritation, vision problems, diarrhoea and excretion of dark urine [7]. Some phenolic compounds have been found to accelerate tumour formation, cancer and mutation [8]. They are considered as one of the priority pollutants by the US Environmental Protection Agency [1,9]. World Health Organisation (WHO) has established the maximum permissible concentration of phenol in drinking water as 1 mg L^{-1} [10]. As a result, various studies have been conducted for the removal of phenolic compounds before being discharged to the receiving sink. The treatment of this type of wastewater involves recuperative

*Corresponding author.

techniques such as solvent extraction, adsorption, filtration, precipitation, ion exchange, biological treatment and destructive techniques such as ozonation and oxidation [4,11–15]. Adsorption technology using activated carbon is currently being used extensively for the removal of pollutants from gaseous and liquid phases. The main disadvantages associated with this adsorbent are the high regeneration cost, intraparticle resistance in adsorption process and poor mechanical strength [7,16]. The process of adsorption has an edge due to its sludge free clean operation and removal of phenols from aqueous solutions having dilute or moderate concentrations. Activated carbon, in granular or powdered form is the most widely used adsorbent [17–19]. In spite of good capacity it suffers from several disadvantages. The cost of activated carbon as well as thermal regeneration of spent carbon is expensive, impractical and produces additional effluent and results in a considerable loss of the adsorbent [20–23]. Recently, adsorption has attracted considerable interest especially chemically and thermally stable adsorbent for removal of phenols from industrial wastes. These wastes require little processing to increase their sorption capacity. Various industrial wastes and agricultural materials such as paper mill sludge, coal, dried sewage waste, water hyacinth ash, green macro alga and rice husk ash have been explored for their technical visibility to remove phenols [1,16,24–26].

In the present study, we report the removal of phenol from aqueous solution using polyaniline Sn(IV) silicophosphate (PTSP). The objective of this work was to investigate the effect of various factors such as initial pH of solution, amount of adsorbent, time of contact and concentration of adsorbates and temperature to determine the various isotherms, kinetics, thermodynamic and equilibrium properties of phenol adsorption. Equilibrium adsorption data were fitted to Freundlich and Langmuir adsorption isotherm models. Several characterization techniques were also used in order to determine the applicability of this ion exchange material in the adsorption studies. PTSP has not yet been tested for the adsorption of phenol from aqueous solution and thus its excellent adsorption capacity and technological applications are helpful in pollution control.

2. Experimental

2.1. Reagents and instruments

The main reagents for the synthesis were aniline, potassium persulphate, stannic chloride, sodium silicate and orthophosphoric acid, which is procured from Merck (Darmstadt, Germany). All other reagents and chemicals were of Sigma (St. Louis, MO, USA). Solutions of stannic chloride (0.25 M), orthophosphoric acid (0.25 M) and sodium silicate (0.25 M) were all prepared in demineralized water (DMW), while a 10% solution (v/v) of aniline and 0.10 M potassium persulphate were prepared in a 1 M HCl solution. A stock solution of phenol was prepared (1,000 mg L^{-1}) in ethanol. Solutions were then diluted to (20–100 mg L^{-1}) to concentration in DMW for further study.

2.2. Materials and methods

The main reagents for the synthesis aniline, potassium persulphate, stannic chloride and orthrophosphoric acids were procured from E-Merck (India), and sodium silicate was obtained from CDH (India). Other chemicals and reagents were of analytical grade and used as received without further purification. The solutions of sodium silicate (0.20 M) and orthophosphoric acid (0.20 M) were prepared with DMW and the solution of $SnCl_4$ (0.20 M) was prepared in DMW, while 10% solution (v/v) of aniline and 0.10 M solution of potassium persulphate were prepared in a 1.0 M solution of HCl.

2.3. Synthesis of PTSP

The gel of polyaniline was synthesized using the same method as explained in our previous paper [27]. The inorganic precipitate of Sn(IV) silicophosphate was prepared by mixing 0.20 M solutions of orthophosphoric acid, sodium silicate and stannic chloride steadily with continuous stirring at 25 ± 2˚C for 1 h, whereby a white gel type slurry was obtained. The pH of the solution was maintained by adding a dilute solution of HCl. The resulting white precipitate so formed was kept overnight in the mother liquor for digestion.

The PTSP composite material was prepared by the mixing of inorganic precipitate and polyaniline gel (in 1:1 volume ratio) with continuous stirring for 1 h at 25 ± 2˚C. The resultant dark green gel obtained was kept for 24 h at room temperature for digestion. The supernatant liquid was decanted and the gel was filtered under suction. The excess acid was removed by washing with DMW and the material was dried in an oven at 50 ± 2˚C. The dried material was grounded into small granules, sieved and converted into H^+ form by treating with 1.0 M nitric acid solution for 24 h with occasional shaking intermittently replacing the supernatant liquid with fresh acid. The excess acid was removed after several washings with DMW and

finally dried at 50 ± 2°C in an oven. By applying above chemical route, a number of samples of PTSP composite were synthesized under different conditions of mixing volume ratios, concentration and of reactants with varying pH. On the basis of better ion exchange uptake capacity together with the physical appearance of the beads and percentage yield, one selected sample was selected for detailed studies.

A LabIndia UV-3200 double beam spectrophotometer with 10 mm matched quartz cells was used for spectrophotometric determination. The infrared (IR) spectra were recorded on Fourier transform infrared (FTIR) Spectrometer (Perkin Elmer [1730, USA]) using KBr disc method. An X'Pert PRO analytical diffractometer (PW-3040/60 Netherlands with CuKa radiation l = 1.5418 Å) was used for X-ray diffraction (XRD) measurement. The scanning electron microscopy instrument (SEM; LEO, 435 VF) was used for SEM images of the material at different magnifications. Transmission electron microscopy (TEM) analysis was carried out on a Jeol H-7500.

2.4. Adsorbate

Phenol has the following chemical structure and its molar mass is 94.111. The cross-sectional area ($nm^2\ mol^{-1}$) of phenol is 0.42 nm^2 [28], while its solubility in water (g L^{-1}) at 20°C is 82 [29].

2.5. Adsorption studies

Batch process was used for the adsorption studies. An adsorbent of 0.30 g was placed in a conical flask with 30 mL solution of phenol of concentration (40 ppm) was added and the mixture was shaken in different pH solutions (at pH 1.0, 3.0, 5.0, 7.0, 9.0 and 11.0), contact time (10–210 min) and different temperature (30–50°C) then filtered using Whatman filter 41 and final concentration of pollutant was determined in the filtrate by UV spectrophotometer at wavelength of 270 nm.

2.6. Characterizations of the adsorbent

XRD was used for the identification of nature of solid composite material. SEM was used to identify the surface quality and morphology of the adsorbent before and after adsorption. FTIR was recorded, to identify the binding groups present before and after adsorption on the adsorbent surface and their involvement in adsorption process. TEM images were also recorded for the average particle size of the adsorbent. The N_2 adsorption isotherm of the samples was measured by Brunauer–Emmett–Teller (BET) method with the help of BET surface area analyzer. BET method is the most widely used procedure for the determination of the surface area of solid materials. Surface area = 155.515 m g^{-1}, pore volume = 0.142 cc g^{-1}, pore radius Dv(r) = 15.970 Å, particle size approx 30–50 nm.

2.7. Effect of contact time and initial concentration

Effect of time on the adsorption of phenol was determined separately by analyzing the residual pollutant in the liquid after contact period from 10 to 210 min. Experiments were performed using batch process at room temperature. 250 mg of adsorbent was added to 25 mL solution with various initial concentrations of phenol (20–100 mg L^{-1}). Samples were withdrawn from conical flasks after specified time interval and analyzed for residual phenol content in the filtrate.

2.8. Effect of temperature

The effect of temperature on the adsorption of phenol was studied by fixed volume (30 mL) of the phenol solution and dose of adsorbent (0.3 g) with initial concentration of 40 mg L^{-1} in conical flasks. These flasks were kept in a temperature controlled water bath shaker at different temperatures (30–50°C) for 4 h at 150 rpm to reach the equilibrium and then filtered. The final concentration of the compound in the filtrate from each flask was then determined as described earlier.

2.9. Effect of pH

The experiment was performed by taking 300 mg each of PTSP into six (100 mL) conical flasks. Twenty-five millilitres of 40 mg L^{-1} solutions of phenol were added into it. The pH value of these suspensions was adjusted to 1.0, 3.0, 5.0, 7.0, 9.0 and 11.0 by adding a solution of conc. HCl or NaOH and after equilibrium, the final pH of phenol was determined using pH metre (ELICO-Li, India).

3. Results and discussion

3.1. Characterizations of the adsorbent

The functional groups or the binding sites were identified by FTIR spectra of native and treated adsorbent with a view to understand the surface binding mechanism. Fig. 1(a) and (b) show the FTIR spectra of

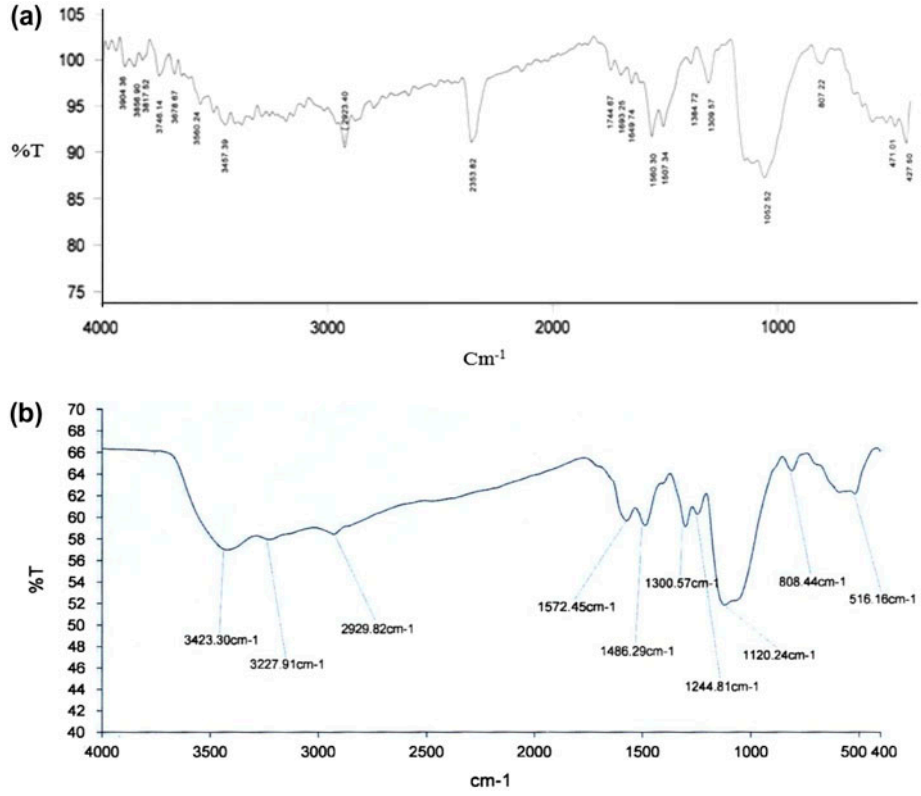

Fig. 1. (a) IR spectra of PTSP before adsorption and (b) after adsorption.

PTSP before and after phenol adsorption and represented the comparison of FTIR spectrum of native and phenol-treated PTSP. The FTIR spectrum of the composite cation-exchanger (Fig. 1(a)) indicates A broadband (in the region 3,457–3,904 cm^{-1}) and a low intensity band at 1,649 cm^{-1} correspond to the presence of interstitial water molecule and free –OH group, respectively [30]. A weak intensity band at 1,560 cm^{-1} is attributed to the presence of secondary aromatic amine although the peak at 1,384 cm^{-1}, and a merged broad band in the range of 1,052–1,309 cm^{-1} are ascribed in plane –CH bending [31]. The bands at ~807 attributed to ν (P = O) [30], ν 427–471 cm^{-1} and ν (Sn–O) vibration [32], respectively.

However, there were some new peaks observed in treated adsorbent showing that adsorption process takes place at the surface of adsorbent. There were shifts in wave number of peaks associated with the treated adsorbent (Fig. 1(b)). The peaks at 1,300 cm^{-1} may be due to deformation vibration of metal hydroxyl group. An assembly of peaks in the region 500–650 cm^{-1} was due to the metal–oxygen stretching vibrations. These shifts in band indicated that there was a high potential for binding process. A clear shift from 1,560 to 1,572 cm^{-1} after phenol treatment was due to C=C stretching. The shift from 1,384 cm^{-1} to 1,300 cm^{-1} assigned to N–O stretch. The peaks at 1,120–1,244 cm^{-1} region in treated adsorbent assigned to C–O stretching vibration. The peaks around 550–470 cm^{-1} showed strong adsorption due to C≡C–H bend.

3.2. Scanning electron microscopy

The SEM analysis gives a sufficient general summary of the surface morphology of the adsorbent. The SEM micrographs of native and phenol-treated PTSP are shown in Fig. 2(a). The morphology of the surface is slightly changed after phenol adsorption (Fig. 2(b)). Adsorbed phenol on the surface of the PTSP can be seen clearly in the form of white patches (Fig. 2(b)). As compared to native (Fig. 2(a)), the surface of adsorbed phenol PTSP is more irregular and porous, which indicates that the surface area and pore volume increased. The distinct morphology is due to the aggregates of phenol deposition, which may briefly indicate that the pores were prominent on the surface of adsorbent before adsorption (Fig. 2(a)) and after the adsorption of phenol, the pores were filled showing adherence of phenol on the surface (Fig. 2(b)) in the

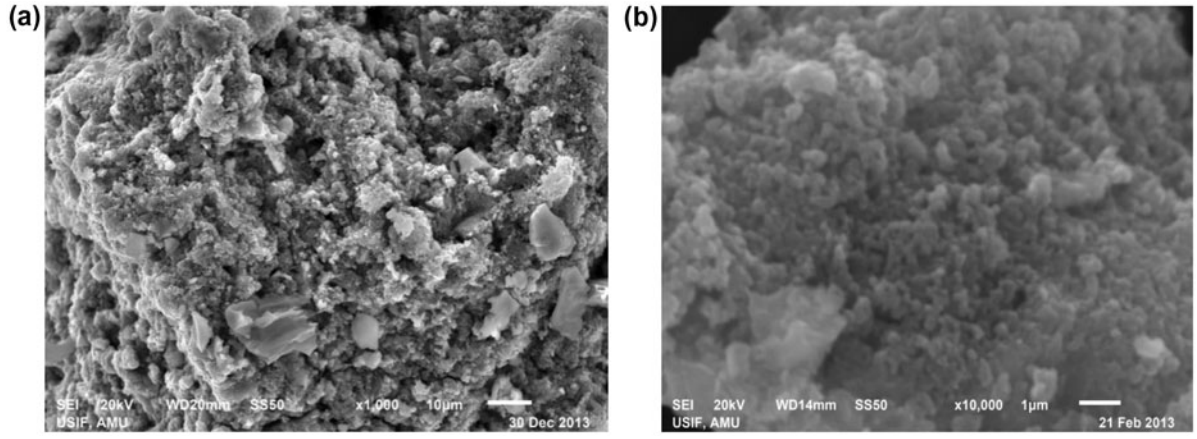

Fig. 2. (a) SEM image of PTSP before adsorption and (b) after absorption.

form of white patches. These large pores and increased surface area are important factors to enhance the intake of phenol.

3.3. Effect of time and initial concentration

The effect of contact time and concentration on the adsorption of phenol are shown in Fig. 3. It has been found that the adsorption is concentration dependent and increased with the increase in initial concentrations. The equilibrium adsorption capacities at 20, 40, 60, 80 and 100 mg L^{-1} initial phenol concentrations were found to be 1.68, 3.92, 5.38, 7.32 and 9.34 mg g^{-1}, respectively. The initial adsorption rate was high for phenol (30 min) and then slowed down while approaching towards equilibrium. The equilibrium time for adsorption of phenols on impregnated fly ash [33], iron marble [34] and peat [35] bagasse fly ash [36], used tea leaves activated carbon [37] and iron oxide coated sand [38] are 2, 1.5,16, 1.5, 3 and 2 h, respectively. The initial adsorption rate of phenol increased with increase in concentration, which might be due to increased driving force and large numbers of vacant surface sites are available for adsorption during the initial stage. With the increase in time, the remaining vacant surface sites are difficult to be occupied due to repulsive forces between the solute molecules on the solid and bulk phases while after saturation of adsorption sites, adsorption of phenol proceeded towards equilibrium through pore diffusion (a slow process). The equilibrium time for the adsorption of phenol was found to be 120 min for 20, 40, 60, 80 and 100 mg L^{-1} initial phenol concentrations.

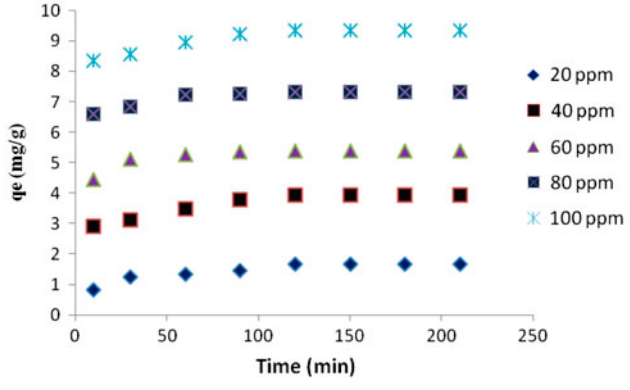

Fig. 3. Effect of contact time on the sorption of phenol on the nanocomposite material at different phenol concentrations.

3.4. Effect of pH

The effect of pH is the most critical parameter which affects the adsorption process and this may be because the charge of both adsorbate and the adsorbent often depends on the pH of the solution. The adsorption of phenol on PTSP was studied in the pH range between 1 and 11. Fig. 4 shows the effect of pH on the phenol adsorption using PTSP under the given conditions. The adsorption capacity increases with the increase in pH (up to pH 5) and then decreased slightly with further increase in the pH (up to pH 11). The optimum adsorption capacity of phenol onto PTSP takes place in the pH region 3–5. A sharp decrease in adsorption capacity was observed up to pH 5, while with further increase in pH, a significant decline in adsorption may be attributed to the formation of phenolate anions. At pH 2, the surface of the adsorbent would be protonated and these led to donor–acceptor interactions between the aromatic rings of the phenol [39]. Effect of pH on batch

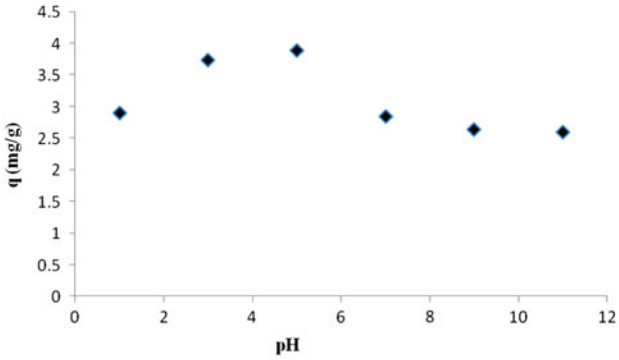

Fig. 4. Effect of pH on the sorption of phenol on nanocomposite PTSP.

adsorption studies of phenol by peat, fly ash and bentonite [35] indicated that phenol was better adsorbed at pH 4.0, 5.0 and 4.0, respectively.

3.5. Adsorption isotherms

In order to optimize the design of adsorption system for the removal of phenol from aqueous solution, it is important to explain the relationship between adsorbed phenol per unit weight of adsorbent (q_e) and residual concentration of phenol in solution (C_e) at equilibrium. Experimental data for the adsorption were fitted in the Langmuir and Freundlich, models at different temperatures and results are reported in Fig. 5 and Table 1. In order to evaluate the fitness of the data, determination coefficient (R^2) for each model.

According to Langmuir model [40], the adsorption occurs on a homogenous surface forming monolayer of adsorbate with constant heat of adsorption for all sites without interaction between adsorbed

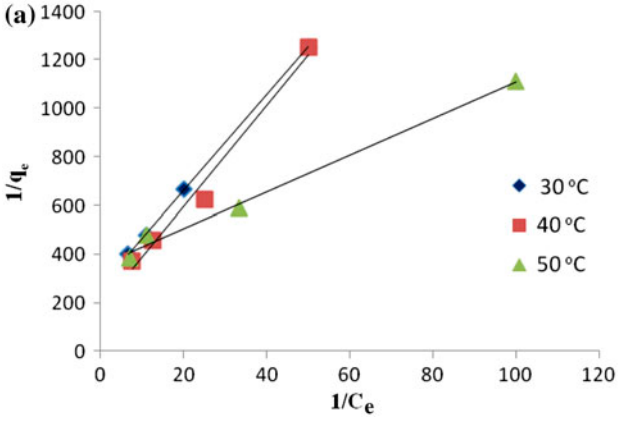

Fig. 5. (a) Langmuir plot and (b) Freundlich plot.

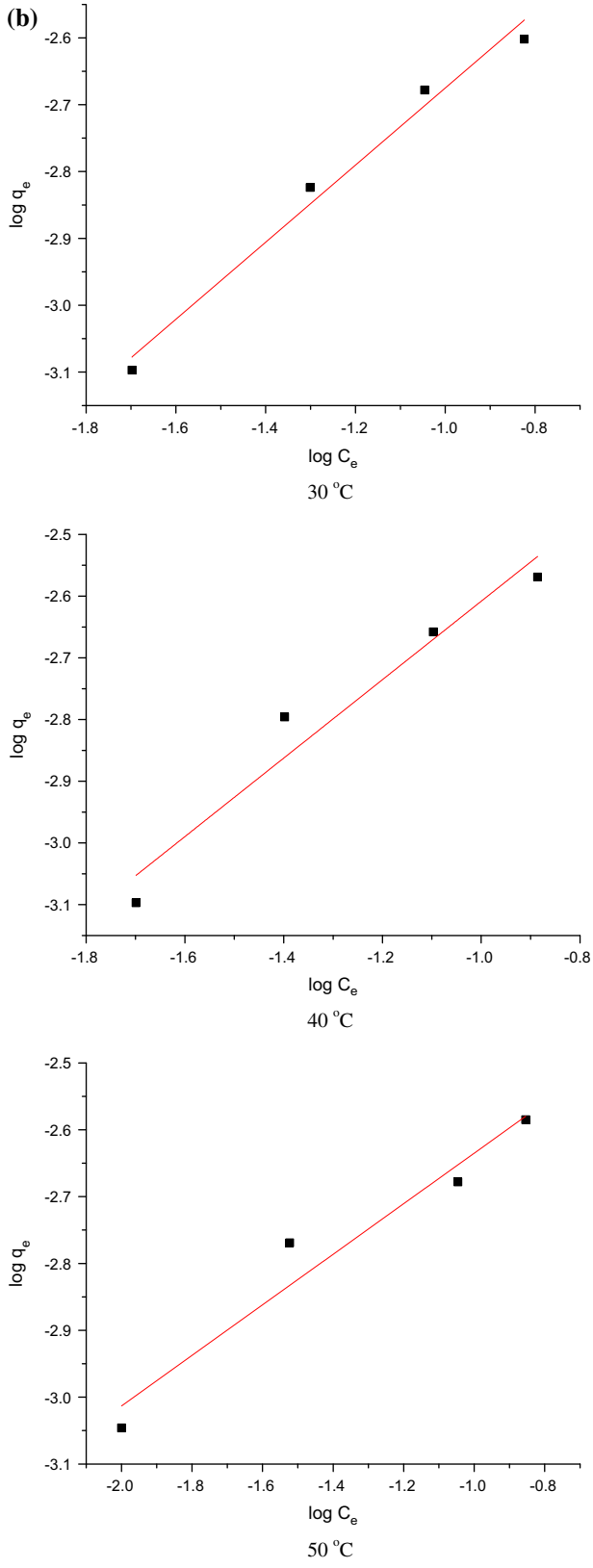

Fig. 5. (*Continued*)

Table 1
Adsorption isotherm parameters for the adsorption of phenol onto PTSP

Isotherms	Parameters	30℃	40℃	50℃
Langmuir	b (L mg^{-1})	13.476	8.593	47.078
	q_m (μg g^{-1})	3.76	5.58	5.82
	R^2	0.9997	0.9839	0.9927
Freundlich	K (mg g^{-1})(L mg^{-1})	0.007982	0.010648	0.00535
	n (g L^{-1})	1.733	1.573	2.645
	R^2	0.9836	0.9533	0.951

molecules [41]. The linear form of Langmuir model may be given as

$$\frac{1}{q_e} = \frac{1}{q_m} \times \frac{1}{b} \times \frac{1}{C_e} + \frac{1}{q_m} \quad (1)$$

where C_e is the equilibrium concentration of phenol in the solution (mg L^{-1}), q_e is the amount of phenol adsorbed per unit weight of adsorbent (mg g^{-1}), q_m is the amount of phenol required to form monolayer (mg g^{-1}) or maximum monolayer adsorption capacity and b is a constant related to energy of adsorption (L mg^{-1}), which represents enthalpy of adsorption and should vary with temperature. In the case of phenol adsorption, plots of $1/q_e$ versus $1/C_e$ at 30, 40 and 50℃ gave straight lines and values of b and q_m were calculated from the slope and intercept of the plots shown in Fig. 5(a). The values of q_m and b increases with increasing temperature indicating a higher heat of adsorption with increasing temperature and the endothermic nature of the adsorption. The data obtained from this model were fitted well at all temperatures as shown by high determination coefficient (R^2), (Table 1).

The Freundlich isotherm model [42] can be applied to multilayer adsorption with non-uniform distribution of adsorption heat and affinities over the heterogeneous surface [43]. The linear form of Freundlich model can be represented as

$$\log q_e = \log K_f + \frac{1}{n} \log C_e \quad (2)$$

where C_e is the equilibrium concentration in mg L^{-1} and q_e shows that the adsorption seems to follow the Freundlich isotherm model as well as Langmuir isotherm, K_f is the Freundlich constant which indicates the relative adsorption capacity of the adsorbent related to bonding energy and n is the heterogeneity factor representing the deviation from linearity of adsorption and is also known as Freundlich coefficient. Plots of log q_e versus log C_e for the adsorption of phenol generated straight lines at 30, 40 and 50℃ and well obeyed at all temperatures as shown in Fig. 5(b). The values of n and K_f have been calculated from the slope and intercept of these plots. The values of Freundlich constant increased with increase in temperature, suggesting that adsorption of phenol is endothermic. The value of n, are higher than one, indicates that adsorption capacity is favoured over the entire range of studied data [44] (Table 1).

The values of E lie between 8 and 16 kJ mol^{-1} and depict the adsorption process follows the chemical ion exchange and if E <8 kJ mol^{-1}, the adsorption process is of a physical nature [45]. In this study, the positive value of energy (E) of adsorption confirms that the adsorption process is endothermic. The higher values of the mean free adsorption energy determined using equation (Table 1) revealed that the adsorption of phenol on PTSP involves physical adsorption due to the van der Waals forces.

It can be concluded that the above models are well fitted for phenol adsorption on PTSP at different temperatures. Table 1 describes the isotherm data of phenol obtained from Langmuir, Freundlich models at different temperatures.

3.6. Thermodynamic study

The effect of temperature on the adsorption of phenol was studied in the temperature range from 30 to 50℃. Thermodynamic parameters such as standard free energy change (ΔG°), standard enthalpy change (ΔH°) and standard entropy change (ΔS°) were estimated using the following relations [46].

$$K_c = \frac{C_{Ad}}{C_e} \quad (3)$$

where K_c is the distribution constant, C_{Ad} and C_e are equilibrium concentrations of target pollutant on the adsorbent and in the solution, respectively. According

to the IUPAC recommendations [47], the distribution constant is defined as the ratio of the concentration of a substance in a single definite form in the extract to its concentration in the same form in the other phase at equilibrium. The Gibbs energy change (ΔG°) indicates the degree of spontaneity of an adsorption process, and a higher negative value reflects a more energetically favourable adsorption. According to thermodynamic law, ΔG° of adsorption is calculated as follows

$$\Delta G^{\circ} = RT \ln K_a \tag{4}$$

where ΔG° is the Gibbs free energy, K_a is the thermodynamic equilibrium constant without units, T is the temperature in Kelvin and R is the gas constant. The values of ΔH° and ΔS° were calculated from the following Van't Hoff equation

$$\ln K_a = -\frac{\Delta H^{\circ}}{RT} + \frac{\Delta S^{\circ}}{R} \tag{5}$$

ΔH° and ΔS° were calculated from the slope and intercept of the plot of log K_a versus $1/T$ (Fig. 6). The values of the thermodynamic parameters are reported in Table 2. These thermodynamic parameters estimate can offer insight into the type and mechanism of an adsorption process (reported in Table 2). Values of free energy change (ΔG°) were negative confirming that adsorption of phenol was spontaneous and thermodynamically favourable since ΔG° of phenol adsorption becomes more negative with increase in temperature, it also reflects whether physiosorption (ΔG° values range from −20 to 0 kJ mol^{-1}) or chemisorption (ΔG° values range from −80 to 400 kJ mol^{-1}). Adsorption of phenol was endothermic as confirmed by positive ΔH° value (Table 2). A positive value of ΔS° for the adsorption of phenol (Table 2) in the temperature range 30–50°C suggests increased in randomness at the adsorbent–adsorbate interface during adsorption since adsorption of phenol dislodge some water molecules from the surface of the adsorbent that resulted increased randomness.

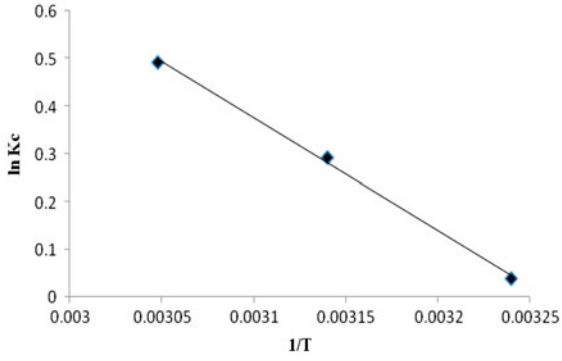

Fig. 6. Van't Hoff plot for the adsorption of phenol onto PTSP.

3.7. Adsorption kinetics

In order to understand mechanism of the adsorption process and to analyze the adsorption rate, the kinetic data were modelled to test experimental data using Lagergren pseudo-first-order [48] and pseudo-second–order [49] equations. The pseudo-first-order expression is given by Eq.

$$\log (q_e - q_t) = -\left(\frac{K_1}{2.323}\right) \times t + \log\ q_e \tag{6}$$

Here q_e is the amount of adsorbate adsorbed per unit weight of adsorbent at equilibrium (mg g^{-1}), q_t is the amount of phenol adsorbed per unit weight of adsorbent at any given time t and K_1 is the rate constant for pseudo-first-order model. The values of K_1 and q_e (cal) were calculated from slope and intercept of the linear plots of log (q_e–q_t) versus t at 40 mg L^{-1} phenol concentration (Fig. 7(a)).

The pseudo-second-order rate expression is used to describe chemisorption involving valency forces through the sharing or exchange of electrons between the adsorbent and adsorbate as covalent forces, and ion exchange [50]. The pseudo-second-order adsorption kinetics rate equation is given as

$$\frac{t}{q_t} = \frac{1}{K_2 \times q_e^2} + \frac{1}{q_e} \times t \tag{7}$$

Here, K_2 (g mg^{-1} min^{-1}) is the adsorption rate constant for pseudo-second-order reaction. The values of K_2 were calculated from the slope of the linear plots of t/q_t versus t at 40 mg L^{-1} phenol concentrations (Fig. 7(b)).

Table 3 provides data of pseudo-first-order rate constants K_1, pseudo-second-order rate constants K_2, the coefficient of determination (R^2), calculated equilibrium adsorption capacity q_e (cal) and experimental equilibrium adsorption capacity q_e (exp). It was found that q_e values calculated from pseudo-first-order kinetic model q_e (cal) at various initial phenol concentrations differed appreciably from the experimental values q_e (exp) showing that system follow pseudo-first-order model. In pseudo-second-order kinetic model the q_e (cal) were not close to q_e (exp) values at

Table 2
Thermodynamic parameters at different temperatures for the adsorption of phenol

Temperature (°C)	ln K_a	ΔG° (kJ mol^{-1})	ΔH° (kJ mol^{-1})	ΔS° (kJ mol K^{-1})	R^2
30	0.03822	−0.09787	45.122	0.147	0.998
40	0.29102	−0.7694			
50	0.4902	−1.3367			

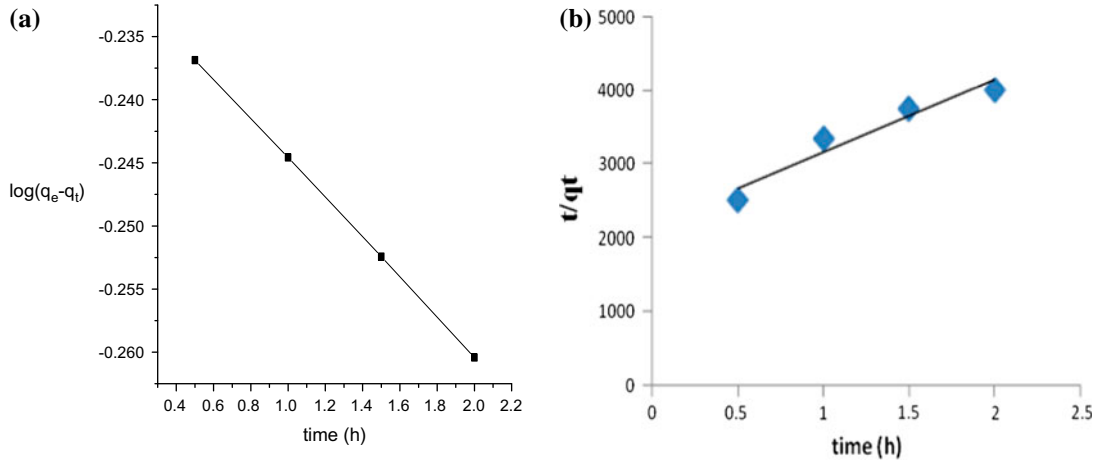

Fig. 7. (a) Pseudo-first-order plot and (b) Pseudo-second-order plot.

Table 3
Pseudo-first order and pseudo-second order rate constants for adsorption of phenol

Concentration (mg L^{-1})	Pseudo-first-order kinetics				Pseudo-second-order kinetics		
	K_1 (min^{-1})	q_e (cal) (mg g^{-1})	R^2	q_e (exp) (mg g^{-1})	q_e (cal) (mg g^{-1})	K_2 (g mg^{-1} min^{-1})	R^2
10	0.03647	0.5902	0.9999	0.62	0.00101695	0.254	0.932

initial phenol concentrations as compared to pseudo-first-order model. The high values of determination coefficient (R^2) also indicate that pseudo-first-order model is better obeyed by the system.

4. Conclusions

A novel nanocomposite has been synthesized by sol-gel method and its adsorption properties have been explored using batch process. The results show that PTSP possessed good adsorption ability for phenol. FTIR, SEM, TEM and XRD analysis demonstrated that the synthetic material is the original design goals. The optimum pH for the adsorption is 3–5. Thermodynamic parameters indicate endothermic and spontaneous nature of adsorption. The mean free energy value shows that adsorption is physical in nature. Langmuir and Freundlich isotherm models are well fitted as indicated by regression coefficient. The kinetic data proved that pseudo-first-order kinetics is applicable model since q_e values calculated from the model are very close to q_e determined experimentally. Hence, synthesized PTSP is an effective adsorbent and can be utilized to reduce phenol concentration from aqueous solution prior to its disposal.

Acknowledgement

The authors are thankful to the UGC for providing financial support. The Research facilities provided by the Department of Chemistry A.M.U., Aligarh are gratefully acknowledged.

References

[1] M.T. Uddin, M.S. Islam, M.Z.J. Abedin, Adsorption of phenol from aqueous solution by water hyacinth ash, J. Eng. Appl. Sci. 2 (2007) 1–11.

[2] M. Ahmaruzzaman, Adsorption of phenolic compounds on low-cost adsorbents: A review, Adv. Colloid Interface Sci. 143 (2008) 48–67.

[3] H. Yamasaki, Y. Makihata, K. Fukunaga, Preparation of crosslinked β-cyclodextrin polymer beads and their application as a sorbent for removal of phenol from wastewater, J. Chem. Technol. Biotechnol. 83 (2008) 991–997.

[4] S. Lin, R. Juang, Adsorption of phenol and its derivatives from water using synthetic resins and low-cost natural adsorbents: A review, J. Environ. Manage. 90 (2009) 1336–1349.

[5] A.Y. Okasha, G.H. Ibrahim, Phenol removal from aqueous systems by sorption of using some local waste materials, EJEAF Che 9 (2010) 796–807.

[6] R.C. Devi, C.A. Sastry, Toxicity of phenols to fish, Indian J. Environ. Protect. 7 (1987) 271–283.

[7] N. Siva Kumar, M. Venkata Subbaiah, A. Subba Reddy, A. Krishnaiah, Biosorption of phenolic compounds from aqueous solutions onto chitosan-abrus precatorius blended beads, J. Chem. Technol. Biotechnol. 84 (2009) 972–981.

[8] A.C.J. Buikema, M.J. McGinniss, J. Cairns, Phenolics in aquatic ecosystems: A selected review of recent literature, Mar. Env. Res. 2 (1979) 87–181.

[9] J. Yan, W. Jianping, B. Jing, W. Daoquan, H. Zongding, Phenol biodegradation by the yeast *Candida tropicalis* in the presence of *m*-cresol, Biochem. Eng. J. 29 (2006) 227–234.

[10] P. Kumaran, Y.L. Paruchuri, Kinetics of phenol biotransformation, Water Res. 31 (1996) 11–22.

[11] Z. Aksu, Equilibrium and kinetic modelling of cadmium(II) biosorption by *C. vulgaris* in a batch system: Effect of temperature, Sep. Purif. Technol. 21 (2001) 285–294.

[12] F. Banat, B. Al-Bashir, S. Al-Asheh, O. Hayajneh, Adsorption of phenol by bentonite, Environ. Pollut. 107 (2000) 391–398.

[13] S. Rengaraj, S.H. Moon, R. Sivabalan, B. Arabindoo, V. Murugesan, Agricultural solid waste for the removal of organics: Adsorption of phenol from water and wastewater by palm seed coat activated carbon, Waste Manage. 22 (2002) 543–548.

[14] N. Roostaei, F.H. Tezel, Removal of phenol from aqueous solutions by adsorption, J. Environ. Manage. 70 (2004) 157–164.

[15] B.H. Hameed, A.A. Rahman, Removal of phenol from aqueous solutions by adsorption onto activated carbon prepared from biomass material, J. Hazard. Mater. 160 (2008) 576–581.

[16] R. Aravindhan, J.R. Rao, B.U. Nair, Application of a chemically modified green macro alga as a biosorbent for phenol removal, J. Environ. Manage. 90 (2009) 1877–1883.

[17] B.W. Dussert, G.R. Van Stone, The biological activated carbon process for water purification, Wat. Eng. Manage. 141 (1994) 22–24.

[18] T. Nakamura, S. Tanada, N. Kawasaki, J. Izawa, T. Tokimoto, Adsorption characteristics of trichloroethylene on plasma-treated activated carbon, Toxicol. Environ. Chem. 47 (1995) 213–222.

[19] Y. Jun, W. Yunxiu, Study on activated carbon in chromium-containing wastewater treatment by XPS, J. Environ. Sci. 6 (1994) 173–179.

[20] J.W. Hassler, Purification with Activated Carbon, Chemical Publishing Co., 1974.

[21] J.R. Perrich, Activated Carbon Adsorption for Wastewater Treatment, CRC Press, 1981.

[22] C. Brasquet, J. Roussy, E. Subrenat, P. Cloirec, Adsorption of selectivity of activated carbon fibres application to organics, Environ. Technol. 17 (1996) 1245–1252.

[23] C.M. Ferro-Castilla, Chemical and thermal regeneration of activated carbon saturated with chlorophenols, J. Chem. Technol. Biotechnol. 67 (1996) 183–189.

[24] N.E. Calace, E. Nardi, B.M. Petronio, M. Pietroletti, Adsorption of phenols by papermill sludges, Environ. Pollut. 118 (2002) 315–319.

[25] A. Gundogdu, C. Duran, H.B. Senturk, M. Soylak, D. Ozdes, H. Serencam, M. Imamoglu, Adsorption of phenol from aqueous solution on a low-cost activated carbon produced from tea industry waste: Equilibrium, kinetic, and thermodynamic study, J. Chem. Eng. Data 57 (2012) 2733–2743.

[26] A.H. Mahvi, A. Maleki, A. Eslimi, Potential of rice husk and rice husk ash for phenol removal in aqueous systems, American J. Appl. Sci. 1 (2004) 321–326.

[27] S.A. Nabi, Md. Shahadat, R. Bushra, M. Oves, F.Ahmed, Synthesis and characterization of polyanilineZr(IV)sulphosalicylate composite and its applications (1) electrical conductivity, and (2) antimicrobial activity studies. Chem. Eng. J. 173 (2011) 706–714.

[28] www.merck-chemicals.com.

[29] K. László, A. Szűcs, Surface characterization of polyethyleneterephthalate (PET) based activated carbon and the effect of pH on its adsorption capacity from aqueous phenol and 2,3,4-trichlorophenol solutions, Carbon 39 (2001) 1945–1953.

[30] C.N.R. Rao, Chemical Applications of Infrared Spectroscopy, Academic Press, New York, NY, 1963.

[31] R.M. Silverstein, G.C. Bassler, T.C. Morrill, Spectrometric Identification of Organic Compounds, fourth ed., John Wiley and Sons, New York, NY, 1981, p. 111 (Chapter 3).

[32] K. Nakamoto, Organometallic and Bioinorganic Chemistry, sixth ed., John Wiley and Sons, New York, NY, 1986, p. 154.

[33] B.K. Singh, N.M. Mishra, S.N. Rawat, Sorption characteristics of phenols on fly ash and impregnated fly ash, Indian J. Environ. Health 36 (1994) 1–7.

[34] D.K. Singh, A. Mishra, Removal of organic pollutants by the use of iron(III) hydroxide-loaded marble, Sep. Sci. Technol. 28 (1993) 1923–1931.

[35] T. Virarghavan, F. de Maria Alfaro, Adsorption of phenol from wastewater by peat, fly ash and activated carbon, Indian J. Environ. Health 40 (1998) 169–176.

[36] M.M. Swamy, I.D. Mall, B. Prasad, I.M. Mishra, Sorption characteristic of o-cresol on bagasse fly and activated carbon, Indian J. Environ. Health 40 (1998) 67–78.

[37] D.K. Singh, B. Srivastava, Removal of some phenols by activated carbon developed from used tea leaves, J. Ind. Pollut. Control 16 (2000a) 19.

[38] D.K. Singh, B. Srivastava, P. Yadav, Iron oxide coated sand as an adsorbent for separation and removal of phenols, Indian J. Chem. Technol. 9 (2002) 285–289.
[39] X.L. Chai, Y.C. Zhao, Adsorption of phenolic compound by aged-refuse, J. Hazard. Mater. 137 (2006) 410–417.
[40] I. Langmuir, The constitution and fundamental properties of solids and liquids. Part I. Solids, J. Am. Chem. Soc. 38 (1916) 2221–2295.
[41] M. Helen Kalavathy, L.R. Miranda, *Moringa oleifera*—A solid phase extractant for the removal of copper, nickel and zinc from aqueous solutions, Chem. Eng. J. 158 (2010) 188–199.
[42] H.M.F. Freundlich, Over the adsorption in solution, J. Phys. Chem. 57 (1906) 385–470.
[43] A.W. Adamson, A.P. Gast, Physical Chemistry of Surfaces, sixth ed., Wiley Interscience, New York, NY, 1997.
[44] A. Tabak, E. Eren, B. Afsin, B. Caglar, Determination of adsorptive properties of a Turkish Sepiolite for removal of Reactive Blue 15 anionic dye from aqueous solutions, J. Hazard. Mater. 161 (2009) 1087–1094.
[45] F. Helfferich, Ion Exchange, McGraw-Hill, New York, NY, 1962, pp. 166.
[46] Y. Liu, Is the free energy change of adsorption correctly calculated?, J. Chem. Eng. Data 54 (2009) 1981–1985.
[47] IUPAC, Compendium of Chemical Terminology, second ed., Blackwell Science, Oxford, UK, 1947.
[48] S. Lagergren, About the theory of so called adsorption of soluble substances, Kung. Sven. Vetensk. Adam. Handl. 24 (1898) 1–39.
[49] Y.S. Ho, G. McKay, The kinetics of sorption of divalent metal ions onto sphagnum moss peat, Water Res. 29 (2000) 297–305.
[50] Y.S. Ho, G. McKay, A comparison of chemisorption kinetic models applied to pollutant removal on various sorbents, Process Saf. Environ. Prot. 6 (1998) 332–340.